

Using Tau Polarization for Charged Higgs Boson and SUSY searches at LHC

Monoranjan Guha^a, D. P. Roy^b

^a Department of High Energy Physics,
Tata Institute of Fundamental Research,
Homi Bhabha Road, Mumbai - 400005, India.

^b Homi Bhabha's Centre for Science Foundation
Tata Institute of Fundamental Research
V.N. Purav Marg, Mumbai-400088, India.

The polarization can be easily measured at LHC in the 1-prong hadronic decay channel by measuring what fraction of the τ -jet momentum is carried by the charged track. A simple cut requiring this fraction to be > 0.8 retains most of the $P = +1$ τ -jet signal while suppressing the $P = -1$ τ -jet background and practically eliminating the fake background. This can be utilized to extract the charged Higgs signal. It can be also utilized to extract the SUSY signal in the stau NLSP region, and in particular the stau co-annihilation region.

1. Introduction

It is easy to measure polarization P as it is reflected in the kinematic distribution of its decay products. Moreover, the best channel for measuring polarization is also the best channel for identification, i.e. the 1-prong hadronic decay channel. In particular a simple kinematic cut, requiring the single charged prong to carry $> 80\%$ of the hadronic τ -jet momentum retains most of the $P = +1$ τ -jet events, while suppressing the $P = -1$ τ -jet background and practically eliminating the fake background from standard hadronic jets. Interestingly the most important channel for charged Higgs boson search at LHC is its decay channel, $H^\pm \rightarrow \tau \nu_\tau$, giving $P = +1$. Similarly a very important part of the parameter space of the minimal supergravity (mSUGRA) model has \tilde{B}^0 as the lightest superparticle, while the next to the lightest one is a stau ($\tilde{\tau}_1$) with a dominant $\tilde{\tau}_R$ component. In this case one expects the supersymmetric (SUSY) signal at LHC to contain a $P = +1$ τ from the cascade decay of squarks and gluinos via $\tilde{\tau}_1 \rightarrow \tau \tilde{B}^0$. In both cases one can use the above kinematic cut to enhance the $P = +1$ signal over the $P = -1$ background as well as the fake background.

The paper is organised as follows. In section 2 we summarise the formalism of polarization in the 1-prong hadronic decay channel and discuss how the above mentioned kinematic cut retains most of the detectable $P = +1$ τ -jet signal while suppressing the $P = -1$ τ -jet as well as the fake τ -jet backgrounds. Section 3

briefly introduces the SUSY search programme at LHC via SUSY as well as SUSY Higgs (and in particular H^\pm) signals. In section 4, we describe the most important H^\pm signal in both $m_H < m_t$ and $m_H > m_t$ regions, which contains a hard τ with $P = +1$ from the above mentioned H^\pm decay. In section 5 we show Monte Carlo simulations using the above kinematic cut for extraction of the H^\pm signal at LHC for both the $m_H < m_t$ and $m_H > m_t$ regions. In the latter case we also briefly discuss a corresponding kinematic cut for extracting the m_H signal in the 3-prong hadronic decay channel of H^\pm . In section 6 we briefly describe the SUSY signal coming from the above mentioned cascade decay process. We also emphasize a very important part of the SUSY parameter space, called the stau co-annihilation region, where the signal contains a soft τ with $P = +1$. In section 7 we show the use of the kinematic cut for extracting the SUSY signal at LHC in the 1-prong hadronic τ -decay channel, with particular emphasis on the stau co-annihilation region.

2. Polarization:

The best channel for τ -polarization is its 1-prong hadronic decay channel, accounting for 50% of its decay width. Over 90% this comes from

$$\tau \rightarrow \nu_\tau \pi (12.5\%); \tau \rightarrow \nu_\tau \rho (26\%); a_1 (7.5\%); \quad (1)$$

where the branching fraction for π and ρ include the small K and K^* contributions, which have identical polarization effects [1]. The CM angular distributions of

decay into and vector meson $v(= \rho; a)$ is simply given in terms of its polarization as

$$\frac{1}{v} \frac{d}{d \cos \theta} = \frac{1}{2} (1 + P \cos \theta)$$

$$\frac{1}{v} \frac{d}{d \cos \theta} \rho_{L,T} = \frac{\frac{1}{2} m^2; m_v^2}{m^2 + 2m_v^2} (1 \pm P \cos \theta) \quad (2)$$

where L,T denote the longitudinal and transverse polarization states of the vector meson. The fraction x of the laboratory momentum carried by its decay meson, i.e. the (visible) π -jet, is related to the angle θ via

$$x = \frac{1}{2} (1 + \cos \theta) + \frac{m^2}{2m_v^2} (1 - \cos \theta); \quad (3)$$

in the collinear approximation ($p \approx m$). It is clear from eqs. 2 and 3 that the relatively hard part of the signal ($P = +1$) π -jet comes from the ρ_L and a_{1L} contributions, while for the background ($P = -1$) π -jet it comes from the ρ_T and a_{1T} contributions [2]. Note that this is the important part that would pass the p_T threshold for detecting π -jets.

One can simply understand the above feature from angular momentum conservation. For $R_{(L)} \rightarrow L; v_{=0}$ it favors forward (backward) emission of or longitudinal vector meson, while it is the other way around for transverse vector meson emission, $R_{(L)} \rightarrow L; v_{=1}$. After boosting back to the laboratory frame the forward emitted meson becomes the leading particle, giving a hard π -jet.

Now the ρ_T and a_{1T} decays favor equal sharing of the momentum among the decay pions, while the ρ_L and a_{1L} decays favor unequal sharing, where the charged pion carries either very little or most of the π -jet momentum. Thus plotted as a function of the momentum fraction carried by the charged pion,

$$R = \frac{p}{p_{jet}}; \quad (4)$$

the longitudinal ρ and a_1 contributions peak at very low or high R (< 0.2 or > 0.8), while the transverse contributions peak in the middle [2, 3]. This is shown in Fig. 1 [3]. Note that the ρ_L contribution would appear as a delta function at $R=1$ in this figure. The low R peaks of the longitudinal ρ and a_1 contributions are not detectable because of the minimum p_T requirement on the charged track for π -identification ($R > 0.2$). Now moving the R cut from 0.2 to 0.8 cuts out the transverse ρ and a_1 peaks, while retaining the detectable longitudinal peak along with the single ρ_L contribution. Thanks to the complementarity of these two sets of contributions, one can effectively suppress

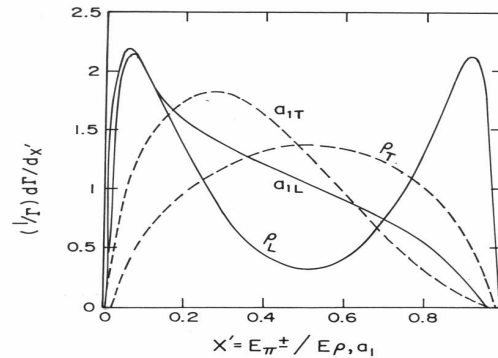


Figure 1. Distributions of $\rho; a$ events in the fractional hadron (π -jet) energy-momentum carried by the charged prong $X^0 = R$ [3],[4]. Note that ρ_L contribution corresponds to a delta function at $X^0 = 1$

the former while retaining most of the latter by a simple cut on the ratio

$$R > 0.8; \quad (5)$$

Thus one can suppress the hard part of the π -jet background ($P = -1$) while retaining most of it for the detectable signal ($P = +1$), even without separating the different meson contributions from one another [3]. This is a simple but very powerful result particularly for hadron colliders, where one cannot isolate the different meson contributions to the π -jet in (1). The result holds equally well for a more exact simulation of the π -jet including the nonresonant contributions. It should be noted here that the simple polarization cut (5) suppresses not only the $p = -1$ π -jet background, but also the fake π -jet background from common hadronic jets. This is particularly important for π -jets with low p_T threshold of 15-20 GeV, as we shall need for SUSY search in the stau co-annihilation region in section 7. Imposing this cut reduces the fake efficiency of hadronic jets from 5-10% level to about 0.2%. The reason is that a common hadronic jet can fake an 1-prong π -jet by a rare fluctuation, when all but one of the constituent particles (mostly pions) are neutral. Then requiring the single charged particle to carry more than 80% of the total jet energy requires a second fluctuation, which is even rarer.

3. SUSY and SUSY Higgs searches at LHC

The minimal supersymmetric standard model (MSSM), has been the most popular extension of the standard model (SM) for four reasons. It provides (1) a natural solution to the hierarchy problem of the

electroweak symmetry breaking (EWSB) scale of the SM, (2) a natural (radiative) mechanism for EWSB, (3) a natural candidate for the dark matter of the universe in terms of the lightest superparticle (LSP), and (4) unification of the gauge couplings at the grand unification (GUT) scale. Therefore, there is a great deal of current interest in probing this model at LHC. This is based on a two-prong search strategy. On the one hand we are looking for the signal of supersymmetric (SUSY) particle production at LHC. On the other hand we are also looking for the signal of the extended Higgs boson sector of the MSSM, and in particular the charged Higgs boson (H^\pm). We shall see below that the $H^\pm \rightarrow \tau^\pm \nu_\tau$ channel plays a very important role for both SUSY and the H^\pm signals and one can use the above mentioned polarization effect in extracting both these signals at LHC.

4. H^\pm Signal

As mentioned above, the MSSM contains two Higgs doublets H_u and H_d , the ratio of whose vevs is denoted by $\tan\beta$. The two complex doublets correspond to 8 degrees of freedom, 3 of which are absorbed as Goldstone bosons to give masses and longitudinal components to the W^\pm and Z bosons. This leaves 5 physical states: two neutral scalars h and H , a pseudo scalar A and a pair of charged Higgs bosons

$$H^\pm = H_u \cos\beta + H_d \sin\beta \quad (6)$$

While it may be hard to distinguish any of these neutral Higgs bosons from that of the SM, the H^\pm pair carry the distinctive hallmark of the MSSM. Hence the H^\pm search plays a very important role in probing the SUSY Higgs sector [4]. All the tree level masses and couplings of the MSSM Higgs bosons are given in terms of $\tan\beta$ and any one of their masses, usually taken to be m_A . It is simply related to m_H via,

$$m_H^2 = m_A^2 + m_W^2 \quad (7)$$

The most important H^\pm couplings are

$$H^\pm \rightarrow \tau^\pm \nu_\tau (cs) : \mp \frac{g}{2M_W} (m_{t(c)} \cot\beta + m_{b(s)} \tan\beta);$$

$$H^\pm \rightarrow \tau^\pm \nu_\tau : \mp \frac{g}{2M_W} m_\tau \tan\beta \quad (8)$$

Assuming the $H^\pm \rightarrow \tau^\pm \nu_\tau$ coupling to remain perturbative up to the GUT scale implies $1 < \tan\beta < m_t/m_b$.

For $m_H < m_t$, eq.8 imply large branching fractions for

$$t \rightarrow bH^\pm \quad (9)$$

decay at the two ends of the above range, $\tan\beta = 1$ and $\tan\beta = m_t/m_b \approx 50$, driven by the m_t and m_b terms respectively. But there is a huge dip in the intermediate region around

$$\tan\beta \approx \frac{P}{m_t - m_b} \approx 7; \quad (10)$$

which is overwhelmed by the SM decay $t \rightarrow bW$. Eq.8 also implies that the dominant decay mode for this H^\pm over the theoretically favored region of $\tan\beta > 1$ is,

$$H^\pm \rightarrow \tau^\pm \nu_\tau; P = +1 \quad (11)$$

where the polarization follows simply from angular momentum conservation, requiring the τ to be right handed. It implies the opposite polarization for the SM process

$$W^\pm \rightarrow \tau^\pm \nu_\tau; P = -1 \quad (12)$$

since the τ is now required to be left-handed. One can use the opposite polarizations to distinguish the H^\pm signal from the SM background [2, 3]. In particular one can use the kinematic cut, mentioned in the introduction, to enhance the signal/background ratio and extend the H^\pm search at LHC over the intermediate $\tan\beta$ range (10), which would not be possible otherwise [3].

For $m_H > m_t$, the dominant production process at LHC is the LO process

$$gb \rightarrow tH^\pm + h.c. \quad (13)$$

The dominant decay channel is $H^\pm \rightarrow \tau^\pm \nu_\tau$, which has unfortunately a very large QCD background. By far the most viable signal comes from the second largest decay channel (11), which has a branching fraction of $\approx 10\%$ in the moderate to large $\tan\beta$ (> 10) region. The largest background comes from $t\bar{t}$ production, followed by the decay of one of the top quarks into the SM channel (12). One can again exploit the opposite polarizations to enhance the signal/background ratio and extend the H^\pm search to several hundreds of GeV for $\tan\beta > 10$ [5, 6, 7]. This will be discussed in detail in the next section.

5. Polarization in the H^\pm search

A parton level Monte Carlo simulation of the H^\pm signal in the $m_H < m_t$ region [3] showed that using the polarization cut (5) enhances the signal/background ratio substantially and makes it possible to extend the H^\pm search at LHC over most of the intermediate $\tan\beta$ region (10). This has been confirmed now by more exact simulations with particle level event generators. Fig.2

shows the H discovery contours at LHC using this polarization cut [7]. The vertical contour on left shows H discovery contour via $t \rightarrow bH^*$; $H^* \rightarrow \tau\nu$ decay. The middle dip in the middle shows the remaining gap in this intermediate $\tan\beta$ region.

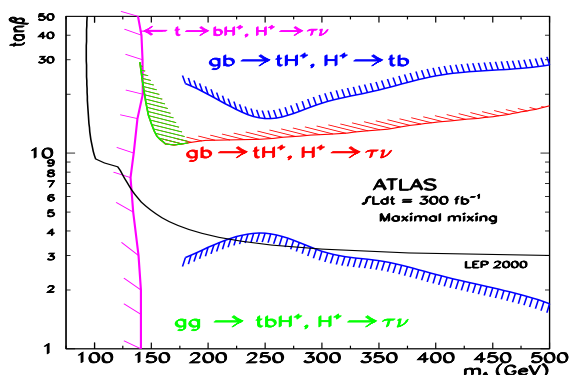


Figure 2. The 5 H boson discovery contours of the ATLAS experiment at LHC from $t \rightarrow bH^*$; $H^* \rightarrow \tau\nu$ (vertical); $gb \rightarrow tH^*$; $H^* \rightarrow tb$ (middle horizontal) and $gb \rightarrow tH^*$; $H^* \rightarrow \tau\nu$ channel [7].

For $m_H > m_t$, the signal comes from (13) and (11), while the background comes from $t\bar{t}$ production, followed by the decay of one top into (12). To start with the background is over two orders of magnitude larger than the signal; but the signal has a harder τ -jet. Thus a $p_T^{\text{jet}} > 100$ GeV cut improves the signal/background ratio. Fig.3 shows the $R(X^0)$ distribution of the resulting signal and background. One can see that increasing the R cut from 0.2 to 0.8 suppresses the background substantially while retaining most of the detectable ($R > 0.2$) signal events. The remaining signal and background can be separated by looking at their distributions in the transverse mass of the τ -jet with the missing p_T , coming from the accompanying ν . Fig.4 shows these distributions from a recent simulation [6] using PYTHIA Monte Carlo event generation [8], interfaced with TAUOLA [9] for handling τ decay. One can clearly separate the H signal from the W background and also measure the H mass using this plot.

Finally, one can also use the polarization effect in the 3-prong hadronic τ -decay channel,

$$\tau \rightarrow \pi^+ \pi^0 \pi^- ; \tau \rightarrow \pi^+ \pi^- \pi^0 \quad (14)$$

with no neutrals. This has a branching fraction of

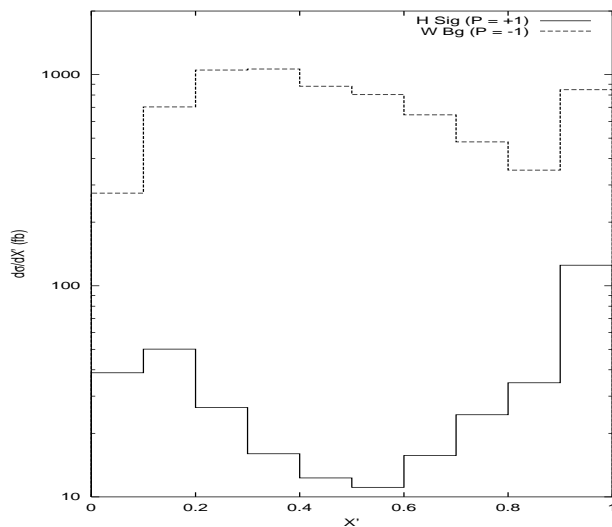


Figure 3. The LHC cross section for a 300 GeV H signal at $\tan\beta = 40$ shown along with the $t\bar{t}$ background in the 1-prong τ -jet channel, as function of the τ -jet momentum fraction $X^0(R)$ carried by the charged pion [4].

10%, which accounts for 2/3rd of inclusive 3-prong τ -decay (including neutrals). Excluding neutrals effectively eliminates the fake τ -jet background from charm on hadronic jets. About 3/4 of the branching fraction for eq.14 comes from a_1 . The momentum fraction R of π^0 channel is equivalent to the momentum fraction carried by the unlike sign pion in a_1 channel. Thus one sees from Fig.1 that one can retain the a_{1L} peak while suppressing a_{1T} by restricting this momentum fraction to < 0.2 , which is accessible in this case. This will suppress the hard τ -jet background events from $P = -1$ while retaining them for the $P = +1$ signal. This simple result holds even after the inclusion of the non-resonant contribution.

Fig.5 shows the H discovery contours of LHC using 1-prong and (1+3)-prong channels [6]. One sees a modest improvement of the discovery reach by including the 3-prong channel. Note also that the 1-prong H discovery contour for 100 fb^{-1} luminosity is consistent with that of Fig.2 for the ultimate 300 fb^{-1} luminosity of LHC.

6. SUSY signal

We shall concentrate in the mSUGRA model as a simple and well-motivated parametrization of the MSSM. This is described by four and half parameters

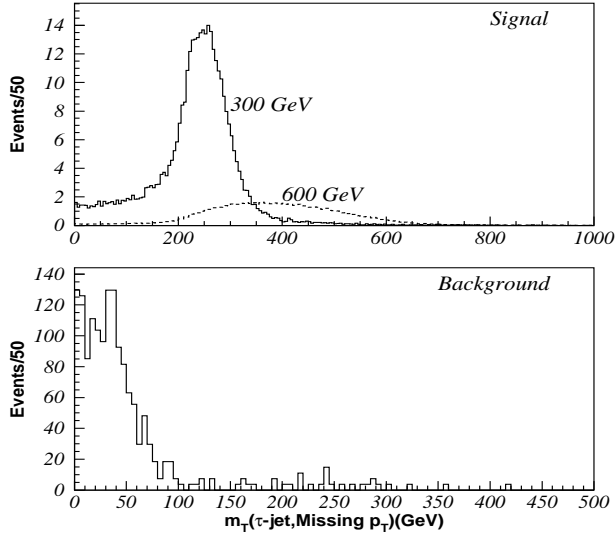


Figure 4. The number of events are shown against transverse mass m_T for signal and background for 1-prong decay channel of τ -jets. These are subject to $p_T^{\text{jet}} > 100 \text{ GeV}$, $R > 0.8$ and $E_T > 100 \text{ GeV}$. The masses of charged Higgs are 300 GeV and 600 GeV and $\tan\beta = 40$. [6].

[10],

$$m_0; m_{1=2}; A_0; \tan\beta \text{ and } \text{sgn}(\mu) \quad (15)$$

the first three representing the common gaugino and scalar masses and trilinear coupling at the GUT scale. The $\tan\beta$ stands for the ratio of the two Higgs vacuum expectation values. The last one denotes the sign of the higgsino mass parameter whose magnitude is fixed by the radiative EW SB condition described below. All the weak scale superparticle masses are given in terms of these parameters by the renormalization group evolution (RGE). In particular the gaugino masses evolve like the corresponding gauge couplings. Thus

$$M_1 = (g_1/g_G) m_{1=2} + 0.4 m_{1=2};$$

$$M_2 = (g_2/g_G) m_{1=2} + 0.8 m_{1=2}; \quad (16)$$

represent the bino \tilde{B} and wino \tilde{W}_3 masses respectively. A very important weak scale scalar mass, appearing in the radiative EW SB condition, is

$$m_{Z'}^2 + M_{Z'}^2 = \frac{M_{H_d}^2 - M_{H_u}^2 \tan^2\beta}{\tan^2\beta - 1}, \quad M_{H_u}^2; \quad (17)$$

where the last equality holds at $\tan\beta > 5$, favored by the Higgs mass limit from LEP [1]. The sign of $M_{H_u}^2$

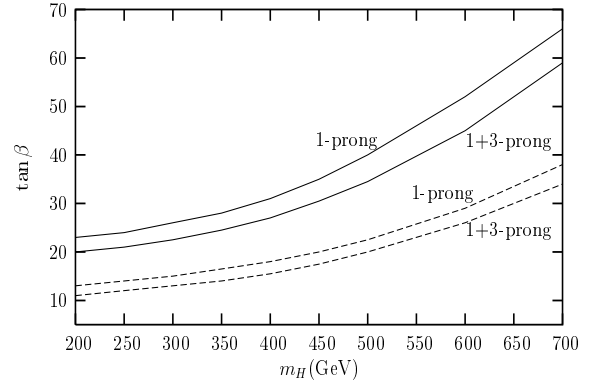


Figure 5. The 5 σ H discovery contours at LHC shown for integrated luminosities of 30 fb^{-1} (solid) and 100 fb^{-1} (dashed) for $H \rightarrow \tau\tau$, with 1 and 3 prong hadronic decay of τ [6].

turning negative by RGE triggers EW SB, as required by (17). The RHS is related to the GUT scale parameters by the RGE,

$$M_{H_u}^2 = C_1(m_0; y_t; \tan\beta) m_0^2 + C_2(m_0; y_t; \tan\beta) m_{1=2}^2$$

$$, \quad m_0^2 + 2m_{1=2}^2; \quad (18)$$

The tiny coefficient of m_0^2 results from an almost exact cancellation of the GUT scale value by a negative top yukawa (y_t) contribution. We see from eq. (16-18) that apart from a narrow strip of $m_0 \gg m_{1=2}$, the mSUGRA parameter space satisfies the mass hierarchy

$$M_1 < M_2 < \mu; \quad (19)$$

Thus the lighter neutralinos and chargino are dominated by the gaugino components

$$\tilde{\chi}_1^0 \sim \tilde{B}; \quad \tilde{\chi}_2^0; \tilde{\chi}_1^\pm \sim \tilde{W}_3; \quad (20)$$

while the heavier ones are dominated by the higgsino. The lightest neutralino $\tilde{\chi}_1^0$ ($\tilde{\chi}$) is the LSP.

The lightest sfermions are the right-handed sleptons, getting only the U(1) gauge contributions to the RGE, i.e.

$$m_{\tilde{\tau}_R}^2 \sim m_0^2 + 0.15 m_{1=2}^2; \quad (21)$$

The Yukawa coupling contribution drives the $\tilde{\tau}_R$ mass still lower. Moreover, the mixing between the $\tilde{\tau}_{L,R}$ states, represented by the off-diagonal term,

$$m_{LR}^2 = m(A + \tan\beta); \quad (22)$$

drives the lighter mass eigenvalues further down. Thus the lighter stau mass eigenstate,

$$\tilde{\tau}_1 = \tilde{\tau}_R \sin\tilde{\alpha} + \tilde{\tau}_L \cos\tilde{\alpha}; \quad (23)$$

is predicted to be the lightest sfermion. Moreover, one sees from eq. 16, 19 and 21 that $\tilde{\nu}_1$ is predicted to be the next to lightest superparticle (NLSP) over half of the parameter space

$$m_0 < m_{1=2} \quad (24)$$

Thanks to the modest $\tilde{\nu}_L$ component in eq.(23), a large part of the SUSY cascade decay signal at LHC proceeds via

$$\tilde{\nu}_1 \rightarrow \tilde{\nu}_1 + \tilde{\chi}_1^0 \quad (25)$$

$$\tilde{\nu}_2^0 \rightarrow \tilde{\nu}_1^0 + \tilde{\chi}_1^0 \quad (26)$$

The dominance of the $\tilde{\nu}_R$ component in $\tilde{\nu}_1$ implies that the polarization

$$P \approx +1; \quad (27)$$

while $P \approx -1$. We shall see in the next section that the polarization effect can be utilized to extract the SUSY signal containing a positively polarized $\tilde{\nu}$ from eq.(25,26).

A very important part of the abovementioned parameter space is the stau co-annihilation region [11], where the \tilde{B} LSP co-annihilates with a nearly degenerate $\tilde{\nu}_1, \tilde{\nu}_1^0$, to give a cosmologically compatible relic density [12]. The mass degeneracy $m_{\tilde{\nu}_1} \approx m_{\tilde{\nu}_1^0}$ is required to hold to 5%, since the freeze out temperature is 5% of the LSP mass. Because of this mass degeneracy the positively polarized lepton coming from eqs.(25,26) is rather soft. We shall see in the next section how the polarization effect can be utilized to extract the soft signal and also to measure the tiny mass difference between the co-annihilating particles.

7. polarization in SUSY search:

The polarization of $\tilde{\nu}$ coming from the $\tilde{\nu}$ decay of eqs.25 and 26 is given in the collinear approximation by [13]

$$P = \frac{a_{11}^R}{a_{11}^R + a_{11}^L} = \frac{(a_{11}^R)^2 - (a_{11}^L)^2}{(a_{11}^R)^2 + (a_{11}^L)^2} \quad (28)$$

$$a_{11}^R = \frac{2g}{\sqrt{2}} N_{11} \tan \beta \sin \alpha - \frac{gm}{2m_W \cos \alpha} N_{13} \cos \alpha$$

$$a_{11}^L = \frac{g}{\sqrt{2}} [N_{12} + N_{11} \tan \beta] \cos \alpha - \frac{gm}{2m_W \cos \alpha} \sin \alpha N_{13}$$

where the 1st and 2nd subscript of a_{ij} refer to $\tilde{\nu}_1$ and $\tilde{\chi}_j^0$; and

$$\tilde{\nu}_1^0 = N_{11}\tilde{B} + N_{12}\tilde{W}_3 + N_{13}\tilde{H}_d + N_{14}\tilde{H}_u \quad (29)$$

gives the composition of LSP. Thus the dominant term is $a_{11}^R \approx \frac{2g}{\sqrt{2}} N_{11} \tan \beta \sin \alpha$, implying $P \approx +1$. In fact in the mSUGRA model there is a cancellation between the subdominant terms, so that one gets $P > 0.9$ throughout the allowed parameter space [14]. Moreover, in the $\tilde{\nu}_1$ NLSP region of eq.(24) $P > 0.95$, so that one can approximate it to $P \approx +1$. The polarization of the $\tilde{\nu}_1^0$ from eq.(26) is obtained from eq.(28) by replacing $a_{11}^{L,R}$ by $a_{1,2}^{L,R}$. The dominant contribution comes from $a_{1,2}^L \approx \frac{g}{\sqrt{2}} N_{22} \cos \alpha$, implying $P \approx -1$. There is a similar cancellation of the subdominant contributions, leading to $P \approx -0.95$ in the $\tilde{\nu}_1$ NLSP region. Thus one can safely approximate $P \approx -1$. Fig.6

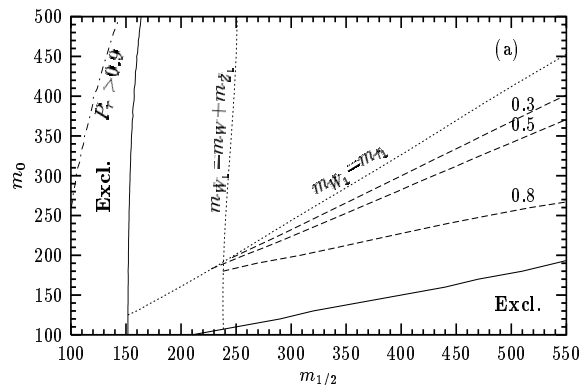


Figure 6. $BR(W_1 \rightarrow \tilde{\nu}_1)$ is shown as contour plots (dashed lines) in m_0 and $m_{1=2}$ plane for $A_0 = 0$, $\tan \beta = 30$ and positive α . The kinematic boundaries (dotted lines) are shown for $W_1 \rightarrow WZ_1$ and $W_1 \rightarrow \tilde{\nu}_1$ decay. The entire region to the right of the boundary (dot-dashed line) corresponds to $P > 0.9$. The excluded region on the right is due to the $\tilde{\nu}_1$ being the LSP while that on the left is due to the LEP constraint $m_{W_1} > 102$ GeV [14]. Note that here W_1 and Z_1 correspond to $\tilde{\nu}_1$ and $\tilde{\chi}_1^0$ in the text.

shows that P is > 0.9 for $\tilde{\nu}_1 \rightarrow \tilde{\chi}_1^0$ decay throughout the mSUGRA parameter space [14]. It also shows that the branching fraction of the decay (25) is large over the $\tilde{\nu}_1$ NLSP region of eq.(24), so that one expects a large part of the SUSY signal in the E_T channel to contain a $\tilde{\nu}$ -jet with $P \approx +1$. Fig.7 shows the R distribution

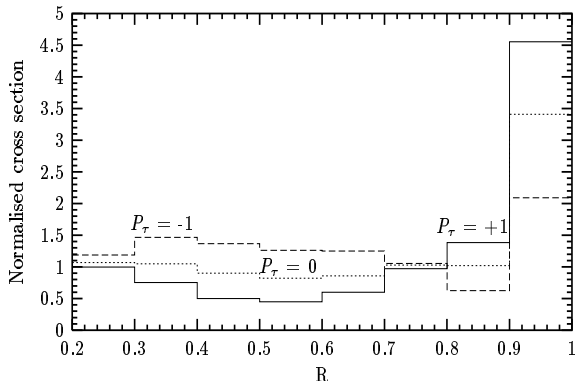


Figure 7. The normalised SUSY signal cross sections for $P = 1$ (solid line), 0 (dotted lines) and -1 (dashed lines) in the 1-prong hadronic τ -jet channel shown as functions of the τ -jet momentum fraction (R) carried by the charged prong [14].

of this $P = +1$ τ -jet at LHC [14]. For comparison the R -distributions are also shown for $P = 0$ and -1 for this τ -jet. Thus one can test the SUSY model or check the composition of $\tilde{\chi}_1^0$ by measuring this distribution.

Let us conclude by briefly discussing the use of polarization in probing the stau co-annihilation region at LSP, corresponding to $m_{\tilde{\chi}_1^0} < m_{\tilde{\tau}_1}$ [15]. This is one of the very few regions of mSUGRA parameter space compatible with the cosmological measurement of the dark matter relic density, and the only one which is also compatible with the muon magnetic moment anomaly [16]. It corresponds to a narrow strip adjacent to the lower boundary of Fig.6, which can be totally covered at LHC. Therefore, the stau co-annihilation region is a region of special interest to the SUSY search programme at LHC. In particular one is looking for a distinctive signature, which will identify the SUSY signal at LHC to this region and also enable us to measure the tiny mass difference between the co-annihilating particles, $M = m_{\tilde{\chi}_1^0} - m_{\tilde{\tau}_1}$. Such a distinctive signature is provided by the presence of a soft ($P = +1$) τ -jet from the $\tilde{\chi}_1^0 \rightarrow \tau \tilde{\chi}_1^0$ decay of eqs.(25,26) in the canonical multijet+ E_T^{miss} SUSY signal. Fig.8 [15] shows the p_T distributions of this soft ($P = +1$) τ -jet signal along with the ($P = -1$) τ -jet background coming mainly from the $\tilde{\chi}_2^0$ decay of eq.(26) and W decay. It also shows a significant fake background from the accompanying hadronic jets in these events. Fig.9 shows that the $R > 0.8$ cut of eq.(5) effectively suppresses the ($P = -1$) background to a little over half the signal size and practically eliminates the fake background.

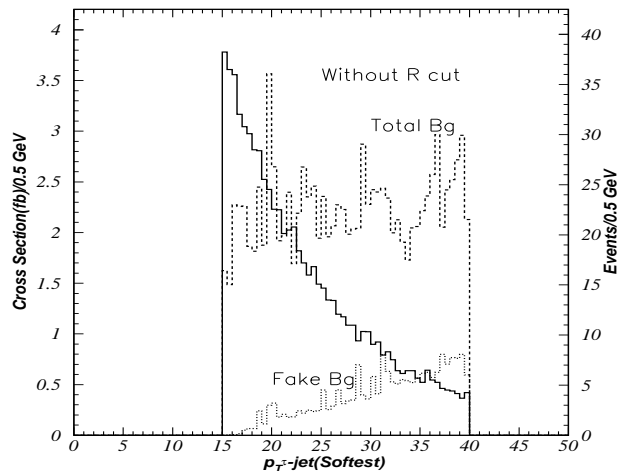


Figure 8. p_T (in GeV) of softest τ -jet for signal and background processes [15].

A distinctive signal with a very steep slope is clearly sticking above the background at the low p_T end. One can use this slope to extract the signal from the background jets at 3 level with a 10fb^{-1} luminosity run of LHC, going upto 10 with luminosity of 100fb^{-1} . Moreover, one can estimate M to an accuracy of 50% at the 1.5 level with 10fb^{-1} , going upto 5 with 100fb^{-1} luminosity [15].

8. Summary

The polarization can be easily measured at LHC in its 1-prong hadronic decay channel by measuring what fraction of the hadronic τ -jet momentum is carried by the charged prong. A simple cut requiring this fraction to be > 0.8 retains most of the detectable $P = +1$ τ -jet events, while effectively suppressing the $P = -1$ τ -jet events and practically eliminating the fake τ -jet events. We show with the help of Monte Carlo simulations that this cut can be effectively used for (1) Charged Higgs boson and (2) SUSY searches at LHC. (1) The most important channel for the H signal at LHC contains a $P = +1$ τ -jet from $H \rightarrow \tau \nu$ decay. The above polarization cut can effectively suppress the $P = -1$ τ -jet background from W decay, while retaining most of the detectable signal ($P = +1$) τ -jet events. So it can be used to extract the H signal at LHC. (2) Over half the mSUGRA parameter space the NLSP is the $\tilde{\chi}_1^0$, which is dominated by the right-handed component, while the

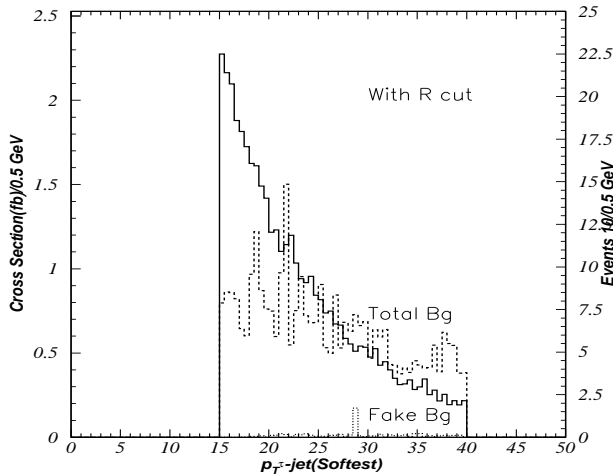


Figure 9. Same as Fig.8, but with R cut (> 0.8) [15].

LSP ($\tilde{\chi}_1^0$) is dominantly bino. In this region a large part of the SUSY cascade decay is predicted to proceed via $\tilde{\chi}_1^0 \rightarrow \tilde{\chi}_1^{\pm} + \gamma$, giving a $P = +1$ $\tilde{\chi}_1^{\pm}$ -jet along with the canonical $\tilde{E}_T + \text{jets}$. One can use the above polarization cut to extract this SUSY signal. A very important part of this region is the co-annihilation region, corresponding to $m_{\tilde{\chi}_1^{\pm}} \approx m_{\tilde{\chi}_1^0}$. So the $P = +1$ $\tilde{\chi}_1^{\pm}$ -jet signal is expected to be soft in this region. However, one can use this polarization cut to extract this signal from the $P = -1$ $\tilde{\chi}_1^{\pm}$ -jet and fake $\tilde{\chi}_1^{\pm}$ -jet backgrounds, and also to measure the small mass difference between the co-annihilating superparticles.

9. Acknowledgement

DPR was supported in part by the BRNS(DAE) through Raja Ramanna Fellowship.

REFERENCES

1. Review of Particle Properties, *J. Phys. G* 33(2006)1.
2. B K Bullock, K Hagiwara and A D Martin, *Phys. Rev. Lett.* 67 (1991) 3055; *Nucl. Phys. B* 395 (1993) 499; D P Roy, *Phys. Lett. B* 277 (1992) 183.
3. S Raychaudhuri, D P Roy, *Phys. Rev. D* 52 (1995) 1556; *Phys. Rev. D* 53(1996) 4902.
4. D P Roy *Mod. Phys. Lett. A* 19 (2004) 1813
5. D P Roy *Phys. Lett. B* 349 (1999) 607.
6. M Guchait, R Kinnunen and D P Roy, *Euro Phys. J.* C 52 (2007) 665.
7. Higgs working group report(Les Houches 2003)K A Assamgou et. al. (hep-ph/0406152).
8. T. Sjstrand, P. Eden, C. Friberg, L. Lonnblad, G. Miu, S. Mrenna and E. Norrbin, *Computer Physics Commun.* 135(2001)238.
9. S. Jadach, Z. Was, R. Decker and J. H. Kuehn, *Comput. Phys. Commun.* 76(1993) 361; P. Golonka et al, hep-ph/0312240 and references therein.
10. For review see, e.g. *Perspectives in Supersymmetry*, ed. G L Kane, world scientific(1998); *Theory and Phenomenology of sparticles*, M. Drees, R M. Godbole and P Roy; World Scientific(2004); *Weak scale Supersymmetry: From super elds to scattering events*, H. Baer and X. Tata, Cambridge UK, Univ. Press(2006).
11. Supersymmetry parameter Analysis; SPA convention and projects, J A. Aguilar-Saavedra et al. *Euro Phys. J. C* 46 (2006) 43. D P Roy, *AIP Conf. Proc.* 939 (2007) 63 (arXiv:0707.1949)[hep-ph].
12. WMAP collaboration, D N Spergel, et. al. *Astrophys. J. Suppl.* 148(2003)175, *Astrophys. J.* 0302209.
13. M M Nojiri, *Phys. Rev. D* 51 (1995) 6281; M M Nojiri, K. Fujii and T. T sukamoto, *Phys. Rev. D* 54 (1996) 6756.
14. M Guchait and D P Roy, *Phys. Rev. D* 54(1996)6756; *Phys. Lett. B* 541(2002)356.
15. R M Godbole, M. Guchait and D P Roy, arXiv:0807.2390[hep-ph].
16. Muon g-2 collaboration, G. Bennet et. al. *Phys. Rev. Lett.* 92(2004) 161802.